ELSEVIER

Contents lists available at ScienceDirect

Atmospheric Environment

journal homepage: www.elsevier.com/locate/atmosenv



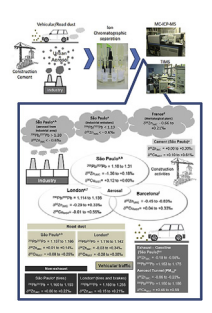
Multi-isotope approach of Pb, Cu and Zn in urban aerosols and anthropogenic sources improves tracing of the atmospheric pollutant sources in megacities



C.E. Souto-Oliveira^{a,b,*}, M. Babinski^a, D.F. Araújo^c, D.J. Weiss^{d,e}, I.R. Ruiz^a

- a Centro de Pesquisas Geocronológicas, Instituto de Geociências, Universidade de São Paulo, Rua do Lago, 562, São Paulo, SP, Brazil
- ^b Environ Finger Solutions Consultoria em Soluções Ltda., Avenida Flora, 463, Apto. 12, Osasco, São Paulo, Brazil
- c Laboratoire de Biogéochimie des Contaminants Métalliques, Ifremer, Centre Atlantique, F-44311, Nantes Cedex 3, France
- d Imperial College London, Earth Science and Engineering, London, SW7 2AZ, UK
- e The Natural History Museum, London, SW7 5PD, UK

GRAPHICAL ABSTRACT



ARTICLE INFO

Keywords: Multi-isotope systems Ion exchange chromatography Pb, Cu, Zn isotopes Non-traditional isotopes Aerosol Reference material Urban pollution Atmosphere Source tracing

ABSTRACT

Studies including multiple isotope systems in aerosols promises unparalleled insights into sources and pathways of metals in the atmosphere. However, such studies remain rare because of the challenges associated with small sample sizes and low analyte masses of the target elements. Here, we present the first study combining accurate and precise determination of Pb, Cu and Zn isotopic ratios in aerosols and anthropogenic materials collected in São Paulo, Brazil. We use a sequential ion chromatography procedure with two different resins for the separation and purification of the analytes. Multi collector mass spectrometry is used for the accurate and precise determination of the isotope ratios. Long term analytical reproducibilities are \pm 0.035 for $^{206}\text{Pb}/^{204}\text{Pb}$, \pm 0.13% for $\delta^{65} \text{Cu}_{\text{NIST}}$ and \pm 0.1% for $\delta^{66} \text{Zn}_{\text{JMC}}$ (\pm 2 σ). Accuracy is assessed using certified reference materials (CRM NIST 2783 aerossol, BRP-1 and others). We analyzed 57 source samples (road dust, tires, cement, road tunnel aerosol) and 113 aerosol samples collected between 2013 and 2015. The results for São Paulo are critically compared with previously published data from studies conducted in São Paulo, London and Barcelona. The key findings are: 1. The isotope signatures for Zn in tires (δ^{66} Zn_{JMC} = 0.16 \pm 0.14, 2 σ , n = 9) and road dust $(8^{66}Zn_{JMC}=0.17~\pm~0.19,\,2\sigma,\,n=13)$ are similar in São Paulo and London suggesting that this isotope system can be used as element specific tracers for non-exhaust traffic. 2. $^{206}\text{Pb}/^{207}\text{Pb}$ vs $\delta^{66}\text{Zn}_{JMC}$ and $\delta^{66}\text{Zn}_{JMC}$ vs δ^{65} Cu_{NIST} multi-isotopic diagrams successfully separate wear off from cars including tires and brakes, car exhaust, industrial emissions and cement sources and improves the discrimination of air pollutant sources. 3. The source identification based on isotope ratios agrees source apportionment based on emissions inventory from these cities. 4. We present Pb, Cu and Zn isotopic data for the first time for the CRM NIST 2783 and BRP-1. These

^{*} Corresponding author. Environ Finger Solutions Consultoria em Soluções Ltda., Avenida Flora, 463, Apto. 12, 06053-040, Osasco, São Paulo, Brazil. E-mail address: carlos.edu.oliveira@usp.br (C.E. Souto-Oliveira).

new data will enable future intercalibration and quality controls in other laboratories. Our study confirms that stable isotope ratio analysis have a great potential for element specific source characterization (e.g., separating non combustion traffic sources from combustion sources) for Cu, Zn and Pb.

1. Introduction

Urban atmospheric pollution is a global environmental problem with prominent effects on public health, due to its link to cancer, cardiovascular, neurological and respiratory diseases, which result in millions of deaths each year (WHO, 2017). Considering the risks of high particulate matter (PM) concentration and the consequential metal species exposure to humans, the identification of air pollutant sources is of great importance to monitoring programs and to policy decisions (Kumar et al., 2014; Saiki at al., 2014; Miranda et al., 2012; Kampa et al., 2008).

In recent years, stable metal isotope ratios have been explored for their potential to improve our understanding of contaminant sources and pathways in the environment, including anthropogenic aerosol emissions from industries, metallurgy and coal plants (Cloquet et al., 2006; Komàrek et al., 2008; Gioia et al., 2008, 2010, 2016; Widory et al., 2004, 2010; Araújo et al., 2017, 2018). Of special interest are the elements Pb, Cu and Zn, since they are important constituents of several man-made materials technological devices whose cycles are drastically altered by anthropogenic activities (Guéguen et al., 2012; Calvo et al., 2013).

The combined study of Pb, Cu and Zn isotope ratios in aerosol samples is hampered due to significant analytical challenges. Aerosol samples collected using active samplers have often small mass and hence contain often only micrograms of aerosol material ($\sim\!100\,\mu g$) and consequently few analyte contents of each element per filter. It makes imperative to optimize protocols to attain lower procedural blanks and prevent sample splitting. A protocol for only Zn isotope ratio determination in aerosol samples was proposed by Gioia et al. (2008) and for Cu and Zn by Dong et al. (2013).

Apart from sample preparation and analyte separation, instrumental fractionation corrections must be performed to avoid artifacts on the isotopic determination of Cu and Zn. Most work to date on instrumental mass fractionation using plasma source mass spectrometers combined with multiple detector arrays has been conducted on first generation instruments (Marèchal et al., 1999; Archer et al., 2004; Mason et al., 2004; Chen et al., 2009; Peel et al., 2008; Sossi et al., 2015; Araújo et al., 2017). The improved ion transmission in the new generations of MC-ICP-MS, which is associated to the combination of Jet sampler with X-skimmer cones design, has reduced instrumental mass fractionation significantly (Albarède et al., 2015; Araújo et al., 2016). However, quantitative transmission of ions is still not achieved and fractionation stability during long-term measurements and intra-session must be assessed to select the appropriate mass bias correction method to eliminate successfully instrumental artifacts.

The aim of this work has been two-fold. First, we wanted to develop and validate an analytical procedure that combines two ion exchange procedures for the simultaneous separation of Pb, Cu and Zn and to assess critically mass bias corrections for subsequent isotopic determinations of Zn and Cu in aerosol, environmental samples (rocks and soil, sediment) and anthropogenic materials (road dust, tires and cement) using a new generation of plasma source mass spectrometers. We included certified reference materials (CRM) of different environmental matrices, including aerosol, rocks, soils, sediment and leaves (BHVO2-basalt, BCR2-basalt, AGV1-andesite, 2709-San Joaquin soil, 1646a-Estuarine sediment, 1573a-Tomato leaves), to validate our method and inedited Pb, Cu and Zn isotopic determinations for NIST-2783 aerosol and BRP reference material (RM). This inedited data is addressed to improve the metrological traceability, data quality control and methodological validation.

Second, we intended to compare the results with previously determined Pb, Cu and Zn isotopic compositions for São Paulo (Gioia et al., 2008, 2016, Souto-Oliveira et al., 2018), London (Dong et al., 2017) and Barcelona (Ochoa and Weiss, 2016), to (i) identify possible city specific differences and (ii) test critically the wider potential for Cu, Zn and Pb isotopic signatures for pollutant tracing and discrimination in urban atmospheres.

São Paulo and London are important megacities with more than 10 million inhabitants with common atmospheric pollutant sources such as vehicular traffic, fossil fuel combustion and road dust suspension. Barcelona is a city with 4.7 million inhabitants with metal sources to atmosphere contrasting to São Paulo and London, namely with higher contribution from industrial activity.

2. Material and methods

2.1. Reagents, certified reference materials and environmental samples

All chemical procedures were conducted in a clean room laboratory (class 10000) and laminar flow hoods (class 100) at the Center of Geochronological Research, University of São Paulo (USP). Ultrapure acids (HCl, HNO3 and HF) were obtained using Teflon still Acid Purification System (Savillex $^{\circ}$, DST-100). Diluted solutions were prepared using Milli-Q ultrapure water (18.2 $\mathrm{M}\Omega\,\mathrm{cm}^{-1}$). Dispensable components (pipette tips, tubes) were washed with HNO3 50% (v v $^{-1}$) solution and ultrapure water prior to their use. PFA Teflon beakers (Savillex $^{\circ}$) were cleaned by boiling in 50% HNO3 and 50% HCl (v v $^{-1}$), separately for 1 h each. In-house ZnUSP and CuUSP solutions were prepared from high purity standard solutions (Merck, CertPur $^{\circ}$) and used as in-house reference standard (USP).

A set of CRMs (BHVO2, BCR1 and BCR2 basalt and AGV1 andesite from USGS, and NIST-2783 aerosol, 2709 San Joaquin soil, 1646a estuarine sediments and 1573a tomato leaves from NIST) and anthropogenic samples (road dust, tires, cement) were selected to develop and validate the analytical procedure, including sample digestion, ion exchange chromatography separation protocol and isotope measurements by MC-ICP-MS and TIMS.

2.2. Sampling and sample dissolution

Aerosol samples, anthropogenic materials (except road dust and tire) and environmental certified materials were dissolved using 4 mL of concentrated HF/HNO $_3$ (2:1) mix in a Savillex $^\circ$ beaker on a hot plate at 120 $^\circ$ C for 3 days. Samples were subsequently dried and re-dissolved in 3 mL 7 M HCl at 120 $^\circ$ C for 24 h. This solution was dried again and then re-dissolved in 1 mL 7 M HCl. This final solution was split in two aliquots for isotope ratio (70%) and elemental (30%) analysis. About 50 mg of road dust and 20 mg of tire were dissolved in concentrated acid mixture (HNO $_3$ /HCl/H $_2$ O $_2$) using a microwave digestion system (Mars 5, CEM corporation) operating with high pressure and temperature-resistant Teflon vessels.

2.3. Elemental analysis

Elemental concentrations of Mg, Al, Ca, Ti, Cr, Fe, Ni, Cu, Zn, Ba and Pb were determined by Q-ICP-MS (X series II, Thermo Scientific). Isotopes of ²⁵Mg, ²⁷Al, ⁴³Ca, ⁴⁹Ti, ⁵²Cr, ⁵⁴Fe, ⁶⁰Ni, ⁶³Cu e ⁶⁶Zn were measured in CCT mode (collision cell technology), whereas ¹³⁷Ba, ²⁰⁶Pb, ²⁰⁷Pb and ²⁰⁸Pb were analyzed in the standard mode. Accuracy and precision were assessed by CRMs (BCR-2, BHVO-2 (basalt) and

NIST-9783 (aerosol)) and SLRS-5 river water which showed coefficient of variations lower than certified value \pm 10%. Total lead concentrations of aerosol samples and CRMs were determined by isotope dilution—thermal ionization mass spectrometry (ID-TIMS) using a Thermo Finnigan MAT 262 mass spectrometer.

2.4. Ion exchange column calibration

2.4.1. Testing ion exchange protocol for Pb, Cu and Zn separation

A protocol was developed combining two ion exchange procedures that enabled the sequential separation of Pb, Cu and Zn. This first procedure includes a column (BIORAD®, 2.0 mL of resin support and 10 mL reservoir) packed with AG MP1 anionic resin for Cu and Zn separation following the elution protocol established by Dong et al. (2013). The second procedure includes a column (an in-house heatshrink Teflon tubing with 4 mm diameter) packed with Bio-Rad[®] AG1-X8 resin and employed to Pb separation as described by Babinski et al. (1999). Before packing the column, the AG-MP1 anionic resin was cleaned with HNO₃ 0.5 M and H₂O, whereas the AG1-X8 anionic resin was washed with H₂O and HCl 6 mol L⁻¹ separately for three times. Fig. 1 illustrates the combined protocol for the sequential separation procedures of Pb, Cu and Zn. In the first column, conditioning, sample loading and matrix elution steps are performed using 4 mL, 1 mL and 1.5 mL 7 M HCl, respectively. Copper elution with 7 M HCl, Fe elution with 2 M HCl and Zn elution with 0.05 M HNO3. Then, the matrix fraction was recovered in a Savillex beaker, dried, dissolved in 0.7 M HBr and processed in the second column. The Bio-Rad® AG1-X8 resin was conditioned in 0.7 M HBr, matrix is eluted using 1.5 mL 0.7 M HBr and Pb eluted using 1 mL 6 M HCl.

2.4.2. Assessing matrix separation and recovery yields

The matrix separation of our protocol was evaluated using elution curves of an unknown aerosol sample and of the CRM BCR-2 basalt. Total recovery during ion exchange chromatography is required to avoid isotope fractionation of Cu and Zn. Thus, recovery yields of Cu and Zn were assessed measuring the isotopic composition and elemental concentrations of Cu and Zn in the artificial solutions, samples and reference materials before and after the chromatography. The artificial solution was composed of analyte (Pb, Cu and Zn) and adding matrix interfering elements (Mg, Al, Ca, Ti, Cr, Fe, Ni, Ba).

2.4.3. Blank contributions

Two types of blanks were assessed: the first one assessed chemical

Table 1

Neptune plus parameters and Faraday cup configuration employed during Cu and Zn isotopic measurements.

Instrumental Parameter	rs	Faraday C	Faraday Collector Configurations			
Coolant Ar flow	16 L min -1	L4	⁶² Ni			
Auxiliary Ar flow	$0.7\mathrm{Lmin^{-1}}$	L3	_			
Sample Ar flow	$1.0 – 1.2 \mathrm{L} \mathrm{min}^{ -1}$	L2	⁶³ Cu			
Glass nebulizer flow	$50 \mu L min^{-1}$	L1	⁶⁴ Zn			
Torch power	1203 W	C	⁶⁵ Cu			
Extraction (hard)	-2,0 V	H1	⁶⁶ Zn			
Sensitivity for Zn	$13 \mathrm{V}\mathrm{ppm}^{-1}$	H2	⁶⁷ Zn			
Sensitivity for Cu	13.5 V ppm ⁻¹	НЗ	⁶⁸ Zn			

dissolution and ion exchange procedures and the second one assessed the aerosol sampling procedure, which included membrane manipulation (weighting, sampling), sample dissolution and ion exchange procedures.

2.5. Method validation of Pb, Cu and Zn isotope measurements

2.5.1. Instrument settings

Copper and zinc isotope measurements were carried out using a MC-ICP-MS Neptune (at University of São Paulo) Plus (double focus system, Thermo Scientific) operated using hard extraction. The sample introduction system was a low-flow nebulizer (50 µL min⁻¹) connected to a Scot double-pass quartz cyclonic spray chamber (wet mode). Data collection was obtained through 40 cycles with 4s integration for standard and sample measurements. Samples were measured bracketed by standards. Instrumental baseline and on peak blank correction were performed with HNO₃ 0.05 mol L⁻¹ solution, using a configuration of 10 cycles with 4s integration, taken before and after samples and standard. The main instrumental parameters and cup configuration are shown in Table 1. 62Ni + was monitored to verify its interference on $^{64}\mathrm{Zn}^{+}$ mass, but the signal was always negligible (~10⁻⁵ V). Results are reported relative to the isotopic certified international standard for Zn (IRMM-3702, JMC (Lyon)) and Cu (NIST-976 and AE633) (eqs. (1) and (2)), which were previously calibrated against our in-house standard references, named Zn_{USP} and Cu_{USP} solutions. Instrumental fractionation was corrected using external normalization and is discussed in the following sections.

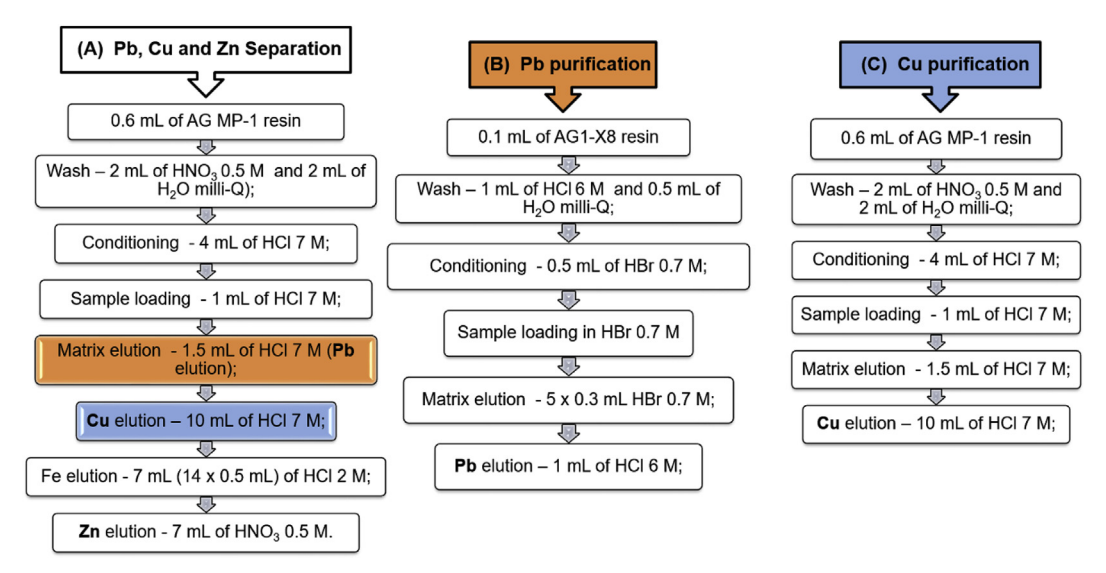


Fig. 1. A. Protocol of sequential ion exchange chromatography for Pb, Cu and Zn B. A second column employed for Pb purification of matrix elution fraction obtained in A. procedure C. A second passage of through the column of Cu fraction collected in A to eliminate residual matrix elements.

$$\delta^{65}Cu(\%_{o}) = \left(\frac{\binom{65}{C}u/\binom{63}{C}u}_{sample}}{\binom{65}{C}u/\binom{63}{C}u}_{standard}} - 1\right)$$
(1)

$$^{66}Zn(\%) = \left(\frac{(^{66}Zn/^{64}Zn)_{sample}}{(^{66}Zn/^{64}Zn)_{standard}} - 1\right)$$
(2)

The Pb isotope ratios were determined by Thermal Ionization Mass Spectrometer (TIMS) using a Thermo Finnigan MAT 262. The dry samples were deposited onto Re filament with ultrapure gel silica $0.25~M~H_3PO_4$. Mass fractionation was corrected using the annual average of 0.095% a.m.u. $^{-1}$, obtained by measurements of NBS-981 (n = 78).

2.5.2. Instrumental fractionation corrections for Cu and Zn isotopes

Instrumental mass fractionation (or mass bias) corresponds to the variable transmission of ion beam in the spectrometer, which result in inaccuracies in isotope ratios measurements (Albarède and Beard, 2004). To correct it, techniques such as sample standard bracketing and external normalization are employed. Briefly, during the sample standard bracketing (d-SSB) approach, samples are measured between two standard runs, assuming that samples and standards fractionate to the same degree during analytical session. This assumption does not account to temporal fractionation fluctuations that occur between standard and sample measurement (Marèchal et al., 1999). In the external normalization, the instrumental fractionation (f) is monitored using a dopant element, which is assumed to have similar fractionation of the analyte. Zinc is commonly used for Cu correction and vice-versa. Different mathematical approaches derived from the exponential law have been proposed: the modified sample standard bracketing (m-SSB), exponential sample standard bracketing (en-SSB) and external empirical normalization (EEN) (Marèchal, 1999; Petit et al., 2008; Sossi et al., 2015; Zhu et al., 2015). Details and equations are presented in the

supplementary material.

The extent of instrumental fractionation is influenced by the analyte-dopant (Zn/Cu) ratio and varies for different MC-ICP-MS instruments (Archer et al., 2004; Chen et al., 2009; Araújo et al., 2016). Therefore, analyte-dopant ratio should be assessed in each laboratory context to improve the precision and accuracy of isotope analysis.

In this work, we investigate the instrumental fractionation behavior concerning the analyte-dopant ratio and the best mass bias corrections procedure. To this end, we assess the precision and accuracy obtained by the use of direct sample standard bracketing (d-SSB) and the different external normalization techniques. The precisions and accuracy were verified in the in-house standard (USP) and RMs (BHVO-2 and AGV-1), spiked with variable Cu concentrations, from 100 to 600 ppb, in different Cu/Zn ratios, from Cu/Zn = 0.1 to 10. The use of CRMs is an approach more realistic than the use of artificial solution which did not take account matrix effects, and hence, provide a better understanding of analyte dopant ratios on instrumental fractionation of real samples. The signal intensity effects on measurements precision of Zn and Cu isotopic compositions is also assessed and further discussed in supplementary material.

2.5.3. Calibrating in-house reference standards and analysis of aerosol samples, anthropogenic and reference materials

Our in-house references standards were calibrated against the international standards to enable inter-laboratory comparisons. Then, the results for the aerosols, anthropogenic materials and CRMs are reported and compared with literature data to validate the methodology. The precision of results is expressed as a combined precision using standard deviation for a single run (s_r) and run-to-run (s_{rr}) conditions (Magnusson, 2014):

$$s_t = (s_r^2/n + s_{rr}^2)^{1/2} (3)$$

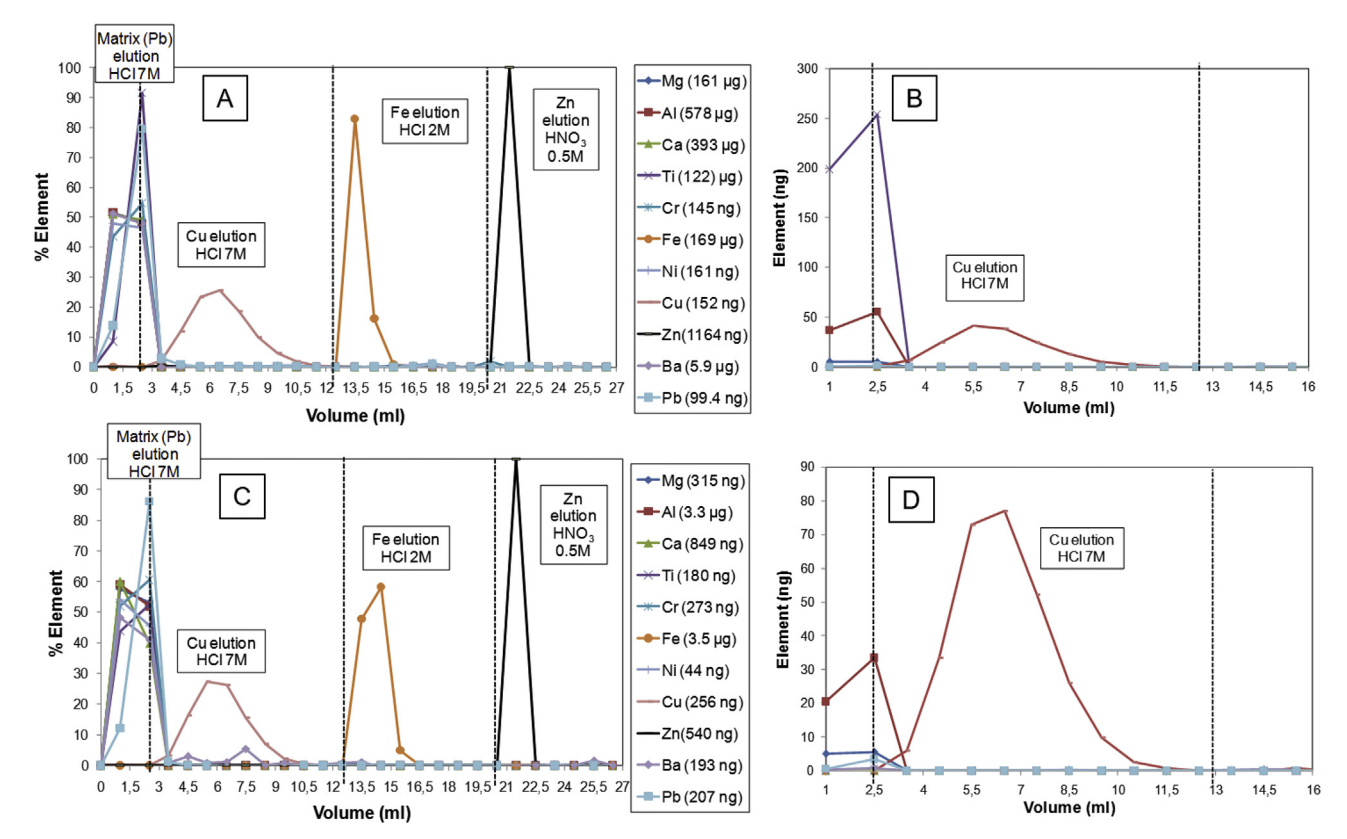


Fig. 2. Elution curves of RM (BRC-2 basalt) (A) and aerosol sample (C). The elemental concentrations of analytes (Pb, Cu and Zn) and interfering elements (Mg, Al, Ca, Ti, Cr, Fe, Ni, Ba) were monitored in a resolution of 1.0 mL. The second Cu purification step of BCR-2 (B) and aerosol sample (D) are also presented. The elemental amounts, present in each sample, submitted to the chromatographic procedure are shown in captions.

3. Results and discussion

3.1. Calibration of ion exchange procedure for sequential separation of lead, copper and zinc

The elution curves obtained for synthetic and true samples using our modified protocol are shown in Fig. 2. The copper fraction was eluted with residual interfering elements (Ti, Al, Mg). The presence of Ti and Al in the Cu fractions may produce oxide and argide polyatomic interferences (24 Mg 40 Ar $^+$; 48 Ti 16 O $^+$, 47 Ti 16 O $^+$, 27 Al 40 Ar $^+$) for Cu and Zn isotopes, and hence must be removed from the Cu fraction before spectrometric measurements (Sossi et al., 2015; Araújo et al., 2016; Chapman et al., 2006). Thus, a second passage of Cu fraction in the column was processed to eliminate totality residual matrix elements (Fig. 2B and D). Interfering elements were not observed in the Zn fractions (Fig. 2A and C).

Analysis of isotope compositions of eluted Cu and Zn fractions showed δ -values about 0 \pm 0.1‰, (2s, n=3), indicating no fractionation during the elution processes. Elemental concentrations measured before and after the ion exchange chromatography confirmed quantitative recoveries of 100 \pm 5% for lead, copper and zinc (Fig. 2A and C). Although isotope fractionation does not occur during ion exchange procedures in the case of Pb, quantitative recovery is a desirable outcome due to the low concentrations (ng) of Pb typically found in aerosol samples.

The procedural blanks related to chemical dissolution and ion exchange procedures are lower than 65 pg for Pb (n = 10), 1 ng for Cu, and 3 ng for Zn. These blanks are lower than those published before for atmospheric particles (Gioia et al., 2008; Dong et al., 2013). To assess the total analytical blank, including membrane filter manipulation (weighting, sampling), sample dissolution and ion exchange procedures, analyses of membranes were performed. Total blank obtained was 87 pg for Pb (n = 5), 2.6 ng for Cu and 5.3 ng for Zn with blank/analyte mass ratio lower than 0.01 for Pb (9 \times 10⁻⁴), Cu (0.008) and Zn (0.009). These results show blank contributions as small as 1%, assuring no appreciable blank effect in the isotopic composition of samples.

3.2. Method validation

3.2.1. Instrumental mass bias

The effect of analyte-dopant ratios (Cu/Zn) on precision and accuracy of δ^{66} Zn_{USP} values was assessed with RMs (BHVO-2 and AGV-1). The slopes obtained empirically with in-house standard solutions ranged from 1.02 to 1.24, showing an increase when Zn > Cu (Fig. 3A). The best precision for ratio measurements was achieved for Zn/Cu = 1 (\pm 0.04‰, 2 σ , n = 5), whereas for the spike/sample ratios of Zn/Cu \neq 1 the precision of the isotope ratio determinations was lower (\pm 0.14‰, 2 σ , n = 4). This was more pronounced for CRMs (Fig. 3B). Since the analyte/dopant = 1 provided the more precise results for our measurements, this ratio was employed in all standards and samples analyzed during this study.

Long-term instrumental fractionation was monitored for two years (2014–2016). Fig. 4A illustrates the slopes of $\ln(r\text{Cu})$ vs $\ln(r\text{Zn})$ plots obtained in several analytical sessions by measurements of Zn and Cu in-house standards (USP). The solutions had concentrations between 300 and 50 ppb and were spiked with Cu— or Zn-dopant in a 1:1 M ratio. The slopes exhibited low variability with an average of $1.02\pm0.15~(\pm2s)$, which agrees within error with the theoretical value (1.02). These long-term investigations under variable conditions using CRMs and international standards ensure the accuracy, precision and robustness of fractionation corrections adopted in our methodology.

The precision (\pm 2 σ) of the main correction methods (d-SSB, en-SSB and EEN) of CRM materials was assessed during selected analytical sessions. The d-SSB method had lower precision (\pm 0.5‰, 2 σ) in each

session compared to EEN (\pm 0.2‰, 2 σ) and en-SSB (\pm 0.05‰) (Fig. 4B). The precision using EEN procedure was dependent of empirical linear fit (R²) in ln (r_{Zn}) x ln (r_{Cu}) plot, which is attained during different Cu and Zn fractionation conditions (Fig. 4C). In session 3, the EEN correction presented similar precision to that achieved for the en-SSB method, as a result of the best linear fit (R² > 0.95) (Fig. 4B).

Table 2 shows that $\delta^{66}Zn_{USP}$ and $\delta^{65}Cu_{USP}$ values for CRMs using en-SSB and EEN corrections varied within \pm 0.05% (expressed as $\Delta_{(en-SSB-EEN)}$). Although, $\delta^{66}Zn_{USP}$ and $\delta^{65}Cu_{USP}$ values for CRMs using m-SSB and en-SSB corrections (expressed as $\Delta_{(en-SSB-EEN)}$) have showed any variation for $\delta^{66}Zn_{USP}$ and small variation within \pm 0.02% for $\delta^{65}Cu_{USP}$. Higher differences (\pm 0.25%) were found between d-SSB and en-SSB. Hence, m-SSB and en-SSB were the best methods. However, the instrumental fractionation of analyte and dopant must be continuously verified in each analytical session. Peel et al. (2008) reported variability of \pm 0.1% for m-SSB, en-SSB and EEN, which are slightly higher compared to our measurements. These variabilities are associated to the inaccuracies in results to assumptions made using the m-SSB ($f_{Zn} \approx f_{Cu}$), EEN and en-SSB ($f_{analyte}/f_{dopant}$).

3.2.2. Calibration of in-house standards

Our in-house standard (USP) were calibrated against the internationally recognized and widely used in-house standard Zn-JMC (Lyon) standard and standard reference IRMM-3702. The Zn-USP standard measured against IRMM showed values of $\delta^{66}\text{Zn}_{\text{USP}/\text{IRMM}} = -0.23 \pm 0.05\%$ (2s, n = 126) (Fig. S1A). With respect to the Zn-JMC (Lyon) standard, measured against IRMM-3702, we obtained a $\delta^{66}\text{Zn}_{\text{JMC}/\text{IRMM}}$ values of $-0.28 \pm 0.05\%$ (2s, n = 36), which is comparable with the values published in the literature (Cloquet et al., 2006; Sossi et al., 2015; Araújo et al., 2016; Petit et al., 2008; Borrok et al., 2010; Moeller et al., 2012). The measurements of Zn-USP against JMC standard yielded Zn_{USP/JMC} = +0.03 \pm 0.04% (2s, n = 30, Fig.

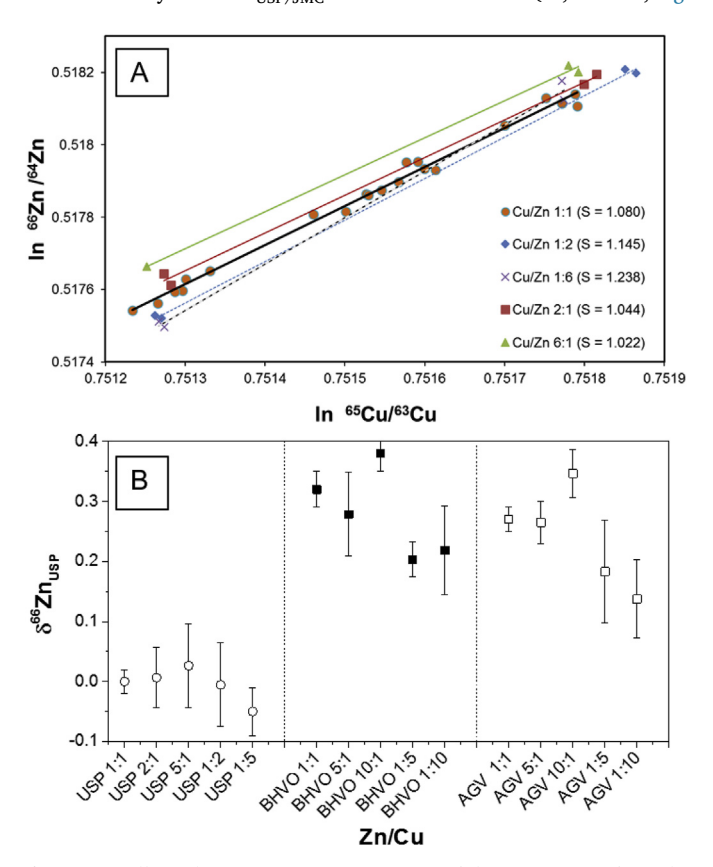


Fig. 3. (A) Effect of Zn/Cu ratios on instrumental fractionation and (B) for fractionation correction to in-house solution and reference materials. The proportions of Cu and Cu concentrations are indicated in the x-axis.

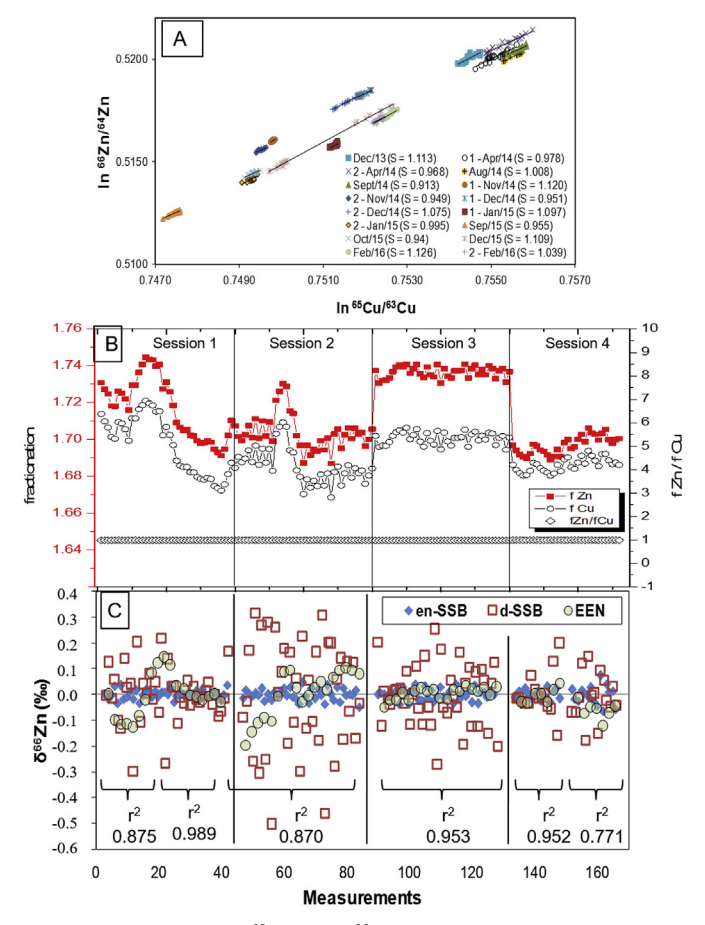


Fig. 4. Three-isotope plot $\delta^{68} Zn_{USP}$ vs $\delta^{66} Zn_{USP}$ representing reference material and aerosol samples. The angular coefficient of the mass fractionation regression line obtained from experimental data (S = 1.961 \pm 0.03) approached the theoretical value (S = 1.942) (Young et al., 2002). All data fell within the 95% confidence limit of the regression line, showing absence of isobaric interference.

S1B). The Cu-USP standard was measured in bracketing to Cu-NIST976 and also Cu-AE633 and the results were $\delta^{65} \text{Cu}_{\text{USP/NIST}} = 0.17 \pm 0.04\%$ (2 σ , n = 15) and $\delta^{65} \text{Cu}_{\text{USP/AE633}} = -0.20 \pm 0.06\%$ (2 σ , n = 15) (Fig. S1C).

3.2.3. Accuracy and precision of Cu, Zn and Pb isotope measurements

Accuracy and precision obtained for CRMs (BHVO. BCR, BHVO, BRP, NIST-2783, 2709-San Jaquin soil, 1646a-Estuarine sediments and 1573a-Tomato leaves) for Cu, Zn and Pb isotope measurements are reported in Tables 3 and 4. Our data showed good agreement with the previously published results in literature (Fig. S2) confirming the accuracy of our methodology. In addition, Pb, Cu and Zn isotopic data

were determined for the first time on the NIST 2783 (δ^{65} Cu_{NIST} $-0.02 \pm 0.02\%$, n=3 and 206 Pb/ 207 Pb = 1.153, n=1) and BRP (δ^{66} Zn_{JMC} = 0.23 \pm 0.05‰, n=4) CRMs.

The combined precision of our methodology was estimated considering the average of combined precision obtained to all RMs (BHVO, BCR, AGV, BRP) and unknown environmental samples measurements (Table S1). The average combined precisions corresponded to \pm 0.035, \pm 0.13‰ and \pm 0.1‰ to $^{206}\text{Pb}/^{204}\text{Pb}$, $\delta^{65}\text{Cu}_{\text{NIST}}$ and $\delta^{66}\text{Zn}$, respectively. The precision and accuracy obtained with our analytical procedure demonstrates that it is adequate to be used for environmental investigations using Pb, Cu and Zn isotopic compositions, such as atmospheric aerosols.

The zinc isotope compositions of aerosol samples and man-made materials, align on the mass-dependent isotopic fractionation line (with slope of 1.96), illustrated in the three-isotope plot of $\delta^{68}\text{Zn}$ vs $\delta^{66}\text{Zn}$ (Fig. 5) (Souto-Oliveira et al., 2018). These results testify no significant matrix effects and, hence, a good purification efficiency of our chromatographic procedure.

3.3. Isotopic signatures of Pb, Cu and Zn in aerosols and potential sources from São Paulo and selected European cities: constrains about anthropogenic sources contributions in urban atmosphere

Recent studies related to Zn and Cu isotope ratios in aerosols from Barcelona and London led to the suggestion that the isotope signature in each city is reflecting different contributions for Cu and Zn from high-temperature processes (combustion) and from non-exhaust traffic emissions (brake and tire wear). We aim to test this hypothesis further by comparing the isotopic signatures of Pb, Cu and Zn of the main sources with those of aerosol collected in São Paulo during this study and comparing them with known emission inventories. Additionally, we test the possible use of a multi-isotope approach to improve the source discrimination.

To this end, we determined the Cu, Zn and Pb isotopic composition in 57 samples of urban sources (fuels, tires, cement, road dust) and 113 aerosol samples collected in the São Paulo city. The aerosol samples containing fine ($PM_{2.5}$) and coarse ($PM_{10\cdot2.5}$) particles were collected for 12 h each, during a period of 1 month in winter of 2013 (Souto-Oliveira et al., 2018). In London, 18 aerosol samples containing coarse particles ($PM_{10\cdot2.5}$), collected each for 48 h during July 2010, and 22 samples of urban sources (vehicular non-exhaust and road furniture) were analyzed and the results published in a previous work ($PM_{10\cdot2.5}$), were collected for 24 or 48 h over a period of 3 weeks during two sampling campaigns in 2012 and 2013 ($PM_{10\cdot2.5}$), were collected for 24 or 48 h over a period of 3 weeks during two sampling campaigns in 2012 and 2013 ($PM_{10\cdot2.5}$).

The Zn isotopic signatures measured in aerosols from São Paulo ($\delta^{66}\text{Zn}_{JMC}=-1.36$ to +0.18%) show a wider range during one month than those measured in PM $_{10}$ aerosol from London ($\delta^{66}\text{Zn}_{JMC}=-0.29$ to +0.33%) sampled during one week and PM $_{2.5}$ aerosols from Barcelona ($\delta^{66}\text{Zn}_{JMC}=-0.83$ to -0.45%) sampled during three

Table 2
Comparison of δ^{66} Zn_{USP} and δ^{65} Cu_{USP} values for rock reference material using different instrumental fractionation correction methods (d-SSB, m-SSB and EEN). Mean was calculated considering m-SSB, en-SSB and EEN and standard deviation (2s). Delta (Δ) values are related to the difference between δ values obtained by different correction methods.

Material	d-SSB	2s	m-SSB	en-SSB	EEN	Mean	2s	$\Delta_{(d\text{-SSB-m-SSB})}$	$\Delta_{(m\text{-SSB-en-SSB})}$	$\Delta_{\text{(m-SSB-EEN)}}$	n
BCR-1	0.35	0.03	0.28	0.28	0.24	0.26	0.03	0.08	0.00	0.04	6
BCR-2	0.32	0.05	0.27	0.27	0.25	0.26	0.04	0.06	0.00	0.02	4
BHVO-2	0.40	0.07	0.33	0.33	0.31	0.32	0.04	0.07	0.00	0.03	4
AGV-1	0.54	0.10	0.28	0.28	0.26	0.27	0.02	0.26	0.00	0.02	2
BCR-1	-0.11	0.29	-0.04	-0.03	-0.06	-0.04	0.12	-0.07	-0.02	0.02	2
BCR-2	-0.09	0.05	0.10	0.10	0.05	0.08	0.12	-0.19	0.00	0.05	3
BHVO-2	-0.25	0.13	-0.14	-0.14	-0.16	-0.15	0.04	-0.11	0.00	0.02	2
AGV-1	-0.23	0.08	-0.19	-0.19	-0.20	-0.19	0.05	-0.05	0.00	0.01	2

Table 3 Comparison of geological reference material to $\delta^{66}Zn_{JMC}$, $\delta^{66}Zn_{IRMM}$ and $\delta^{65}Cu_{NIST976}$ values obtained in this study and reported in the literature. First $\delta^{65}Cu_{NIST976}$ value published to NIST-2783.

Material	Reference	$\delta^{66} Zn_{JMC}$ (‰)	$\delta^{66} Zn_{IRMM}$ (‰)	2s	n	$\delta^{65} Cu_{NIST976}$ (‰)	2s	n
BCR 2	This study	0.29	0.01	0.07	6	0.23	0.11	2
	Archer and Vance (2004)	0.20	_	0.09	12	_	-	_
	Chapman et al. (2006)	0.29	_	0.12	8	_	-	_
	Cloquet et al. (2006)	0.32	_	0.13	2	_	-	_
	Toutain et al. (2008)	0.26	_	0.04	5	_	_	_
	Sonke et al. (2008)	0.25	_	0.04	4	_	_	_
	Herzog et al. (2009)	0.33	_	0.09	2	_	_	_
	Bigalke et al. (2010)	0.23	-0.09	0.08	2	0.19	0.08	1
	Moeller et al. (2012)	0.33	0.04	0.13	3	0.14	0.05	
	Sossi et al. (2015)	0.25	-0.05	0.01	3	0.08	0.05	2
	Araújo et al. (2016)	0.25	-	0.08	10	-	-	-
BCR 1	This study	0.30	0.00	0.09	4	0,11	0.12	2
	Archer and Vance (2004)	0.20	-	0.08	12	0,07	0.08	6
BHVO 2	This study	0.33	0.06	0.06	5	0.08	0.07	2
	Herzog et al. (2009)	0.29	_	0.09	-	-	-	_
	Moynier et al. (2009)	_	_	_	_	0.10	0.07	4
	Moeller et al. (2012)	0.48	_	0.13	3	0.10	0.04	6
	Sossi et al. (2015)	0.27	-0.03	0.06	-	0.01	0.05	2
	Araújo et al. (2016)	0.25	-	0.09	10	-	-	-
BRP	This study	0.23	-0.16	0.05	4	-	-	-
AGV 2	This study	0.27	0.04	0.03	2	-0.02	0.06	2
	Moynier et al. (2009)	_	_	_	-	0,11	0,04	4
	Moeller et al. (2012)	0.50	0.21	0.06	-	0,10	0,11	8
	Araújo et al. (2016)	0.29	-	0.06	2	-	-	-
NIST 2783	This study	0.17	-0.13	0.03	-	-0.02	0.02	-
	Gioia et al. (2008)	0.17	-	0.10	-	-	-	-
2709 San Joaquin Soil	This study	0.29	-	0.10	4	-	-	-
	Araújo et al. (2016)	0.28	-	0.10	4	-	-	-
1646a Estuarine sediment	This study	0.37	-	0.02	3	=	-	-
	Araújo et al. (2016)	0.32	-	0.06	4	_	-	-
1573a Tomato leaves	This study	0.84	-	0.09	2	-	-	-
	Araújo et al. (2016)	0.79	-	0.09	4	-	-	-

Table 4
Comparison of Pb isotopic compositions reported in literature with values obtained in this study for geological reference materials. First Pb isotopic composition published to particulate reference standard (NIST-2783). a - values reported in analytical certifies of RM b- values for residual fraction.

Material	Reference	$^{206}\text{Pb}/^{204}\text{Pb}$	2s	$^{207}\text{Pb}/^{204}\text{Pb}$	2s	$^{208}\text{Pb}/^{204}\text{Pb}$	2s
BCR-2	This study	18.740	0.005	15.600	0.006	38.653	0.007
		18.736	0.010	15.596	0.010	38.638	0.011
		18.744	0.005	15.606	0.006	38.673	0.005
		18.741	0.009	15.604	0.009	38.667	0.010
		18.747	0.015	15.611	0.016	38.696	0.019
	Mean	18.744	0.007	15.604	0.012	38.666	0.044
	USGS ^a	18.750	0.011	15.615	0.003	38.691	0.021
	Collerson et al. (2002)	18.757	0.012	15.623	0.007	38.723	0.018
	Baker et al. (2004)	18.765	0.011	15.628	0.005	38.752	0.022
	Weis et al. (2006)	18.753	0.020	15.625	0.004	38.724	0.041
BHVO-2	This study	18.677	0.026	15.552	0.026	38.310	0.028
	Collerson et al. (2002)	18.679	0.002	15.562	0.002	38.285	0.004
	Baker et al. (2004)	18.649	0.019	15.540	0.017	38.249	0.022
	Weis et al. (2006)	18.647	0.024	15.533	0.009	38.237	0.018
AGV-1	This study	18.909	0.006	15.624	0.006	38.453	0.007
	-	18.902	0.004	15.617	0.005	38.429	0.004
		18.901	0.006	15.616	0.008	38.429	0.007
	Mean	18.904	0.009	15.619	0.009	38.437	0.028
	Weis et al. (2006) ^b	18.900	0.009	15.610	0.010	38.564	0.043
	Weis et al. (2006)	18.940	0.006	15.653	0.004	38.560	0.010
NIST-2783	This study	17.981	0.006	15.596	0.007	37.892	0.006
2709 San Joaquin Soil	This study	19.070	0.017	15.635	0.011	38.831	0.028

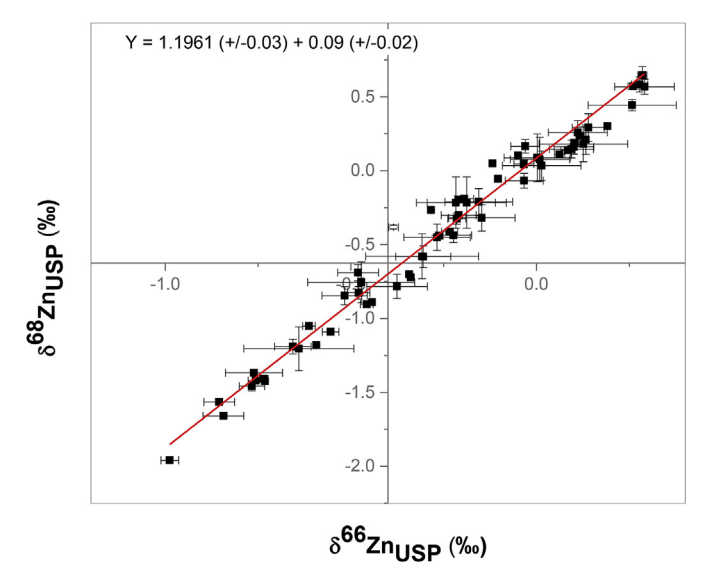


Fig. 5. Long-term and intra-session instrumental fractionation and precision of the main correction methods (d-SSB, en-SSB and EEN). **(B)** Variability of instrumental mass fractionation during two years (2014–2016) of measurements in various analytical sessions. **(C)** Cooper and Zinc fractionations during 4 analytical sessions (8–10 h each) by measurements of international standard solution (300 ppb of Cu NIST976 and Zn IRMM3702). Application of the main fractionation methods correction (en-SSB, d-SSB and EEN) in international standards. For each session, a coefficient of determination (r²) was calculated to constrain the precision of EEN and dependency of linear fit.

weeks (Fig. 6A). Road dust from São Paulo is characterized by isotopically heavy Zn (δ^{66} Zn_{JMC} = -0.03 to +0.34‰), similar to that found in London. The range overlaps well with isotope signatures for Zn in tires and brakes (δ^{66} Zn_{JMC} = 0.00-0.22‰) and with ore concentrates (δ^{66} Zn_{JMC} = -0.04 to +0.30‰) used in industrial manufacturing. This suggests that the heavy Zn isotopic signatures measured in aerosol of these cities can likely be attributed to road dust suspension and non-exhaust sources (Fig. 6A) (Dong et al., 2017; Souto-Oliveira et al., 2018).

Zinc isotopes furthermore enable to differentiate between non-exhausts and exhaust vehicular emissions (Fig. 6A). Exhaust emissions likely display a significantly lighter isotope ratios for gasoline exhaust $(\delta^{66} Zn_{JMC} = -0.18$ to -0.58%, Fig. 6A) and for aerosols collected in road tunnel, which have $\delta^{66} Zn_{JMC}$ values between -0.06 and -0.23% (Gioia et al., 2008; Souto-Oliveira et al., 2018). Aerosols in a roadside tunnel are well known to be composed of sources from non-exhaust and exhaust vehicular traffic (Martins et al., 2006; Brito et al., 2013).

Heavier Zn signatures of road dust and non-exhaust, similar with those observed in ore concentrates, are in line with mechanical process of tire wear, which not produce isotope fractionation (Ochoa et al., 2016; Souto-Oliveira et al., 2018). The light isotope compositions of exhaust vehicular emissions may result of similar mechanisms of isotope fractionation observed in metallurgy industries (Sirvy et al., 2008) and coal-combustion systems (Ochoa and Weiss, 2015), where combustion processes enrich in light isotopes the fuel gas phase following Rayleigh distillation model. Our results are therefore in line with the previous indications that Zn isotopes are a tool for discriminating between Zn emitted during high-temperature processes such as combustion or smelting and low-temperature processes (i.e., abrasion from tires and brakes or electrochemical refining) (Ochoa and Weiss, 2015).

Isotopically lightest Zn was measured in aerosol in São Paulo ($\delta^{66} Zn_{JMC} < -0.60\%$) and in Barcelona ($\delta^{66} Zn_{JMC} < -0.45\%$) and in both studies it was explained with significant contributions from industrial emissions (Fig. 6A) (Ochoa et al., 2016; Souto-Oliveira et al., 2018). This assumption is largely based on previous work that reported light Zn signatures emitted to atmosphere by metal refineries and

metallurgical plants (Mattielli et al., 2009; Yin et al., 2015). Furthermore, association of light Zn signatures with industrial emissions was supported by other geochemical proxies, such as long-range transportation from an important industrial area (Cubatão) in São Paulo and by enrichment factors of Cd and Zn in Barcelona (Gioia et al., 2010; Ochoa et al., 2016; Souto-Oliveira et al., 2018).

The ²⁰⁶Pb/²⁰⁷Pb ratios measured in aerosol (1.16–1.31) and road dust (1.16–1.19) from São Paulo are more radiogenic and more variable than in aerosols from London (1.114–1.136) (Fig. 6B). The radiogenic lead (²⁰⁶Pb/²⁰⁷Pb > 1.20) observed in aerosol from São Paulo are related to emissions from an industrial area (Cubatão; Gioia et al., 2016; Souto-Oliveira et al., 2018). On the other hand, less radiogenic lead found in aerosol and road dust from São Paulo has major contributions of vehicular emissions. Similar observations were derived from Pb isotope measurements in London, which contains Pb provided of nonexhaust, re-mobilized Pb from leaded gasoline and road furniture (Fig. 6B) (Dong et al., 2017; Souto-Oliveira et al., 2018).

Aerosol samples from São Paulo show a similar range in Cu isotope signatures (δ^{65} Cu_{NIST} = -0.01 to +0.55%) like London and Barcelona (Fig. 6C). The signatures observed are in line with those of road dust $(\delta^{65}Cu_{NIST} = -0.28 \text{ to } +0.30\%)$, road furniture $(\delta^{65}Cu_{NIST} = -0.12)$ to +0.55%), vehicular traffic (δ^{65} Cu_{NIST} = +0.46 to +0.59%), nonexhaust $(\delta^{65}Cu_{NIST} = +0.27$ to +0.62%) and cement $(\delta^{65}Cu_{NIST} = +0.10 \text{ to } +0.61\%)$. Positive Cu isotope signatures found in cement agree with signatures typically found in silicates $(\delta^{65}Cu_{NIST} = 0.09 \pm 0.24\%)$, fly ash $(\delta^{65}Cu_{NIST} = +0.11 \pm 0.08\%)$ and other raw materials (i.e. limestone, calcite and gypsum) used for the production of cement (Asael et al., 2007; Bigalke et al., 2010). In previous work, Souto-Oliveira and colleagues have suggested that contributions from cement, vehicular traffic and road dust can be distinguished using Cu isotopes (Souto-Oliveira et al., 2018). In Barcelona, isotopically heavier Cu (δ^{65} Cu_{NIST} = +0.04 to +0.36%) was tentatively associated to non-exhaust emissions based on Cu/Sb ratio in brake wear (4.6 \pm 2.3) and PM₁₀ (6.7–11.6) samples with high vehicular contributions. In opposite, PM_{2.5-80} samples from London collected during winter have showed Cu/Sb ratio between 19 and 31, which was mostly associated to contributions of fossil fuel (Ochoa et al., 2016).

Fig. 7A and B shows distintic fields for aerosol from São Paulo, London and Barcelona using bivariant plots including Cu, Zn and Pb isotopes. These fields are in line with the statement that each city present own "isotopic signature", pointed out by Ochoa et al. (2016).

Similarity of Zn isotopic signatures found in tires (non-exhaust) from São Paulo and London suggest that these source fingerprint may be more general and therefore useful for future air quality models. In addition, industrial emissions in São Paulo city are well separated from vehicular traffic (exhaust and non-exhaust) using Zn isotopes. Contributions from specific industrial area (i.e., Cubatão) are identified using Pb isotopes (Fig. 7A). Metallurgical industries in Cubatão and other areas around São Paulo city are the major source of Zn and Pb emissions. The isotope fields of road furniture, surface tarmac and manhole cover, partially overlap isotopic field of road dust from São Paulo (Fig. 7A), which suggest that these are important sources to be assessed in the future studies in São Paulo (Kumar et al., 2016).

Combining zinc and copper isotope systems in a bivariant plot discriminates between vehicular traffic, road dust and cement from São Paulo (Fig. 7B). Zinc isotope systems differentiate vehicular traffic from road dust, while Cu isotopes discriminate cement from road dust. Aerosols samples from São Paulo, London and Barcelona have similar Cu isotopic signatures (Fig. 6C) but the $\delta^{66} \text{Zn}_{\text{JMC}}$ vs $\delta^{65} \text{Cu}_{\text{NIST}}$ diagram allow to visualize contributions of road dust, road furniture, vehicular traffic, non-exhaust and cement to these aerosol samples.

The sources contributions in aerosol derived using Pb, Cu and Zn isotopes are in line with atmospheric emissions inventory for particulate matter (PM_{10} and $PM_{2.5}$) from São Paulo, London and Barcelona (Fig. 7C) (CETESB, 2013; LAEI, 2010; APICE, 2012). The emission

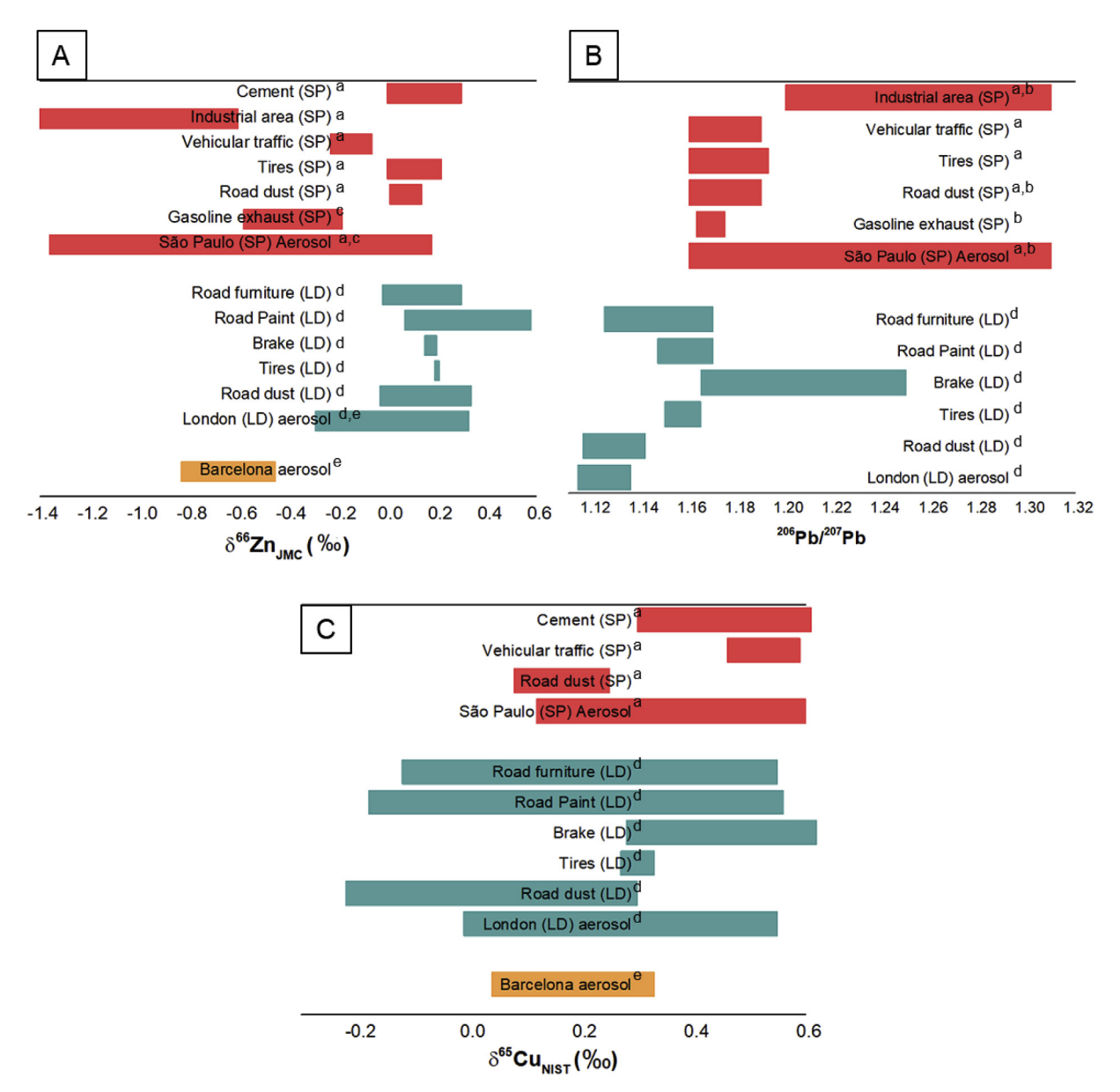


Fig. 6. Comparison of Pb, Cu and Zn isotopic signatures intervals measured on aerosol and urban sources from São Paulo, London and Barcelona cities. (a – Souto-Oliveira et al. (2018), b – Gioia et al. (2017), c – Gioia et al. (2008), d – Dong et al. (2017), e – Ochoa Gonzalez et al. (2016)).

inventories show that vehicular traffic, named as road transport, showed higher contributions in São Paulo and London than in Barcelona and industrial emissions have higher contributions in Barcelona than in São Paulo and London. The emission inventories are described in more detail in Supplementary information. Isotope fingerprints should be an important tool to improve sources identification in emissions inventories and air quality studies. To this end, extensive isotopic characterization of main anthropogenic sources, shown Fig. 7C, must be developed.

Recent studies have supported the relevance of the isotopic systems to trace atmospheric sources in urban, industrial and remote areas (Gioia et al., 2016; Widory et al., 2004, 2010; Sonke et al., 2008; Yin et al., 2015; Souto-Oliveira et al., 2018; Dong et al., 2017; Ochoa et al., 2016), and applying a multi-isotope approach may be the key to discriminate and identify multiple sources in complex systems as the atmosphere.

4. Conclusions

We present an analytical procedure that allows a simultaneous separation and purification of Pb, Cu and Zn elements, followed by isotopic analysis using TIMS and MC-ICP-MS. Efficiency and robustness of our procedure was tested with various complex matrix such as aerosol, environmental samples (rocks, sediments and soil) and anthropogenic materials (tire, cement). The accurate and simple procedure includes a sequential chromatographic separation protocol with recovery yields close to 100% and complete purification of interfering elements matrices. Precision obtained for CRMs and unknown samples (tire, road dust and cement) was ± 0.035 for $^{206}\text{Pb}/^{204}\text{Pb}$ ratios, $\pm 0.1\%$ for $\delta^{66} Zn_{JMC}$ and $\pm~0.13\%$ for $\,\delta^{65} Cu_{NIST}\,$ values. This precision was achieved optimizing several investigations on instrumental fractionation correction, which showed better precision for external normalization and analyte-dopant ratio = 1. Accuracy was assessed using certified reference materials (BCR 1,2 and BHVO2-basalt, AGV 2-andesite, 2783-aerosol, 2709-San Joaquin soil, 1646a-estuarine sediment, 1573a-tomato leaves), which agreed with reported data from other

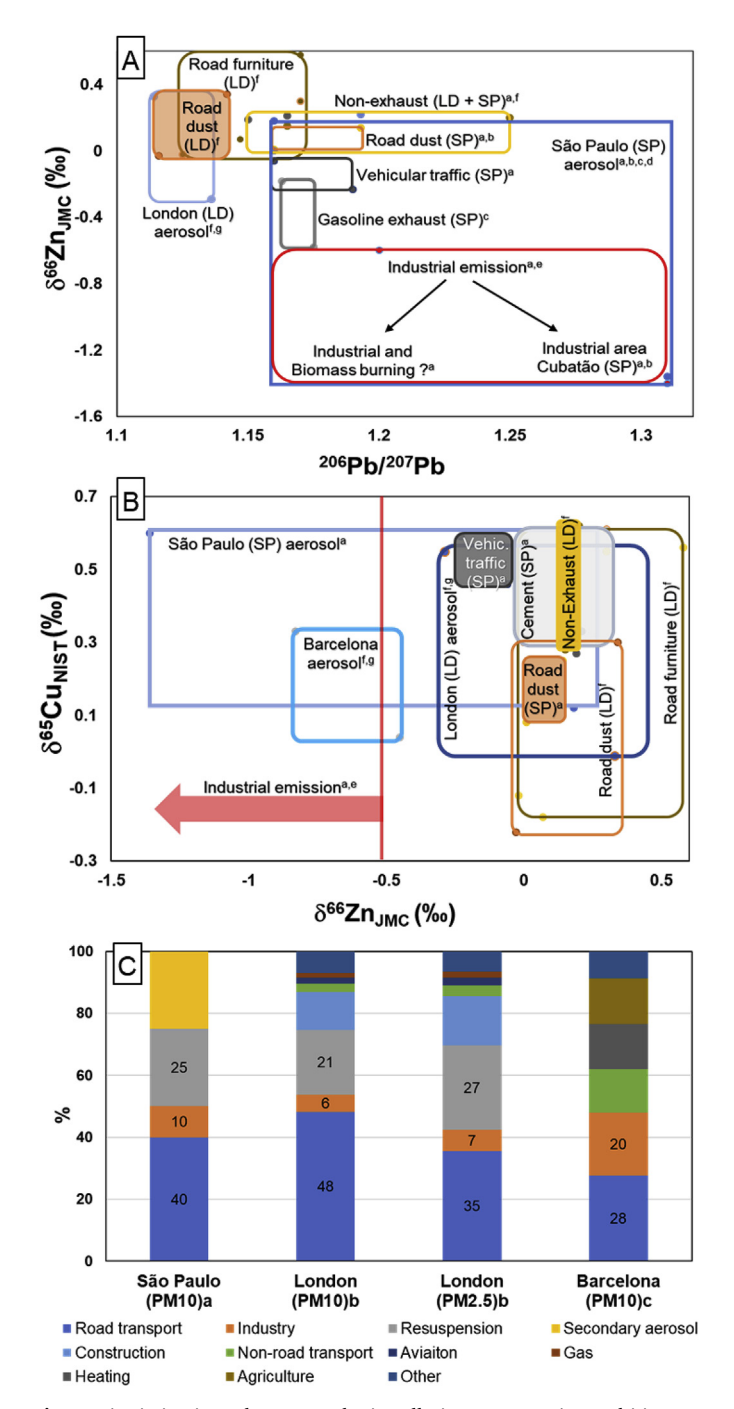


Fig. 7. Discriminating urban atmospheric pollution sources using multi-isotope diagrams and comparison of isotopic fields of the main urban sources and aerosol from São Paulo, London and Barcelona using (A) $^{206}\text{Pb}/^{207}\text{Pb}$ vs $\delta^{66}\text{Zn}_{\text{JMC}}$ diagram and (B) $\delta^{66}\text{Zn}_{\text{JMC}}$ vs $\delta^{65}\text{Cu}_{\text{NIST}}$ diagram. (a – Souto-Oliveira et al. (2018), b – Gioia et al. (2017), c – Gioia et al. (2008), d – Mattielli et al. (2009), e – Dong et al. (2017), f – Ochoa Gonzalez et al. (2016)). (C) Atmospheric inventory emissions of the main particulate matter sources from São Paulo, London and Barcelona. (a – CETESB (2013), b – LAEI (2010) c – APICE (2012)).

laboratories. Furthermore, we report the first Pb and Cu isotopic data on aerosol (NIST-2783) and soil (San Joaquin-2709) RMs and Zn isotopic composition on BRP-1 RM.

The analytical procedure was employed to analyze 57 samples of urban sources (tires, cement, road dust) and 113 aerosol samples from São Paulo city. We compared the isotope signatures of Pb, Cu and Zn in the main urban sources and aerosol from São Paulo, London and

Barcelona using $^{206}\text{Pb}/^{207}\text{Pb}$ vs $\delta^{66}\text{Zn}_{JMC}$ and $\delta^{66}\text{Zn}_{JMC}$ vs $\delta^{65}\text{Cu}_{NIST}$ bivariate plots. In these diagrams, Zn isotopes discriminate between non-exhaust and exhaust traffic and industrial emissions with isotopically positive, slightly negative and negative signatures, respectively. Industrial emissions from São Paulo and road dust from São Paulo and London were successfully separated using Pb isotopes. In addition, vehicular traffic, road dust and cement sources were distinguished by Zn and Cu isotopes. These multi-isotopic diagrams demonstrated as a powerful tool to discriminate between many sources in complex systems as polluted atmospheres in urban areas. However, fractionation process during aerosol transportation in atmosphere must be evaluated in future studies to improve these diagrams.

The Zn isotopic signatures of non-exhaust emissions from São Paulo and London showed similar values, indicating that this isotopic fingerprint possibly is the same in different cities and has potential to be used as reference in future studies. Road dust from London differ from São Paulo city due the less radiogenic isotopic signatures associated to re-mobilized Pb from leaded gasoline, which remains an important source to road dust from London. The positive $\delta^{66} \text{Zn}_{\text{JMC}}$ and $\delta^{65} \text{Cu}_{\text{NIST}}$ values in aerosols from São Paulo and London have similar signatures like vehicular traffic (exhaust + non-exhaust), road dust, road furniture and cement, whereas isotopically negative Zn found in aerosols from São Paulo and Barcelona was associated to industrial emissions.

Our critical comparison of Pb, Cu and Zn isotopes signatures of the sources and aerosol from São Paulo, London and Barcelona are in line with atmospheric inventory emissions of these cities and show that similar anthropogenic sources, as tires from São Paulo and London, follow also similar isotope patterns for specific elements, in some cases, with overlap of isotope signatures. This is an indicative that some anthropogenic sources may present isotope signatures independent of the city.

Acknowledgements

This study is part of a major project entitled "Narrowing the Uncertainties in Aerosol and Climate changes in the state of São Paulo (NUANCE)", funded by the Fundação de Amparo à Pesquisa do Estado de São Paulo. This study was funded further by the Institutos Nacionais de Ciência e Tecnologia (INCT, Science and Technology National Institutes). Carlos Eduardo Souto-Oliveira held a PhD scholarship from the Brazilian Coordenação de Aperfeiçoamento de Pessoal de Nível Superior. The CPGeo staff is acknowledge for providing analytical support during this study.

Appendix A. Supplementary data

Supplementary data to this article can be found online at https://doi.org/10.1016/j.atmosenv.2018.11.007.

References

Albarède, F., Albalat, E., Télouk, P., 2015. Instrumental isotope fractionation in multiplecollector ICP-MS. J. Anal. At. Spectrom. 30, 1736–1742.

Albarède, F., Telouk, P., Blichert-Toft, J., Boyet, M., Agranier, A., Nelson, B., 2004. Precise and accurate isotopic measurements using multiple-collector ICPMS. Geochem. Cosmochim. Acta 68, 2725–2744.

APICE Common mediterranean strategy and local practical actions for the mitigation of port, industries and cities emissions. http://www.apice-project.eu/, Accessed date: 17 May 2018.

Araújo, D.F., Machado, W., Weiss, D., Mulholland, D.S., Garnier, J., Souto-Oliveira, C.E., Babinski, M., 2018. Zinc isotopes as tracers of anthropogenic sources and biogeochemical processes in contaminated mangroves. Appl. Geochem. 95, 25–32.

Araújo, D., Boaventura, G.R., Viers, J., Mulholland, D.S., Weis, D., Araújo, D., Lima, B., Ruiz, I., Machado, W., Babinski, M., Dantas, E., 2016. Ion exchange chromatography and mass bias correction for accurate and precise Zn isotope ratio measurements in environmental Reference Materials by MC-ICP-MS. J. Braz. Chem. 00, 1–11.

Araújo, D.F., Boaventura, G.R., Machado, W., Viers, J., Weiss, D., Patchineelam, S.R., Ruiz, I., Rodrigues, A.P.C., Babinski, M., Dantas, E., 2017. Tracing of anthropogenic zinc sources in coastal environments using stable isotope composition. Chem. Geol. 449, 226–235.

- Archer, C., Vance, D., 2004. Mass discrimination correction in multiple-collector plasma source mass spectrometry: an example using Cu and Zn isotopes. J. Anal. At. Spectrom. 19, 656–665.
- Asael, D., Matthews, A., Bar-matthews, M., Halicz, L., 2007. Copper isotope fractionation in sedimentary copper mineralization (Timna Valley, Israel). Chem. Geol. 243, 238–254.
- Babinski, M., Van Schmus, W.R., Chemale, F., 1999. Pb-Pb dating and Pb isotope geochemistry of Neoproterozoic carbonate rocks from the Sao Francisco basin, Brazil: implications for the mobility of Pb isotopes during tectonism and metamorphism. Chem. Geol. 160. 175–199.
- Baker, J., Peate, D., Waight, T., Meyzen, C., 2004. Pb isotopic analysis of standards and samples using a 207Pb–204Pb double spike and thallium to correct for mass bias with a double-focusing MC-ICP-MS. Chem. Geol. 211, 275–303.
- Bigalke, M., Weyer, S., Kobza, J., Wilcke, W., 2010. Stable Cu and Zn isotope ratios as tracers of sources and transport of Cu and Zn in contaminated soil. Geochem. Cosmochim. Acta 74, 6801–6813.
- Borrok, D.M., Gieré, R., Ren, M., Landa, E.R., 2010. Zinc isotopic composition of particulate matter generated during the combustion of coal and coal + tire-derived fuels. Environ. Sci. Technol. 44, 9219–9224.
- Brito, J., Rizzo, L.V., Herckes, P., Vasconcellos, P.C., Caumo, S.E.S., Fornaro, A., Ynoue, R.Y., Artaxo, P., Andrade, M.F., 2013. Physical–chemical characterisation of the particulate matter inside two road tunnels in the S\u00e3o Paulo Metropolitan Area. Atmos. Chem. Phys. 13, 12199–12213.
- Calvo, A.I., Alves, C., Castro, A., Pont, V., Vicente, A.M., Fraile, R., 2013. Research on aerosol sources and chemical composition: past, current and emerging issues. Atmos. Res. 120, 1–28.
- CETESB, Environmental Protection Agency of São Paulo Estate, 2013. Air quality report for the state of São Paulo. http://ar.cetesb.sp.gov.br/publicacoes-relatorios/, Accessed date: 10 June 2018.
- Chapman, J.B., Mason, T.F.D., Weiss, D.J., Coles, B.J., Wilkinson, J.J., 2006. Chemical separation and isotopic variations of Cu and Zn from five geological reference materials. Geostand. Geoanal. Res. 30, 5–16.
- Chen, J.B., Louvat, P., Gaillardet, J., Birck, J.L., 2009. Direct separation of Zn from dilute aqueous solutions for isotope composition determination using multi-collector ICP-MS. Chem. Geol. 259, 120–130.
- Cloquet, C., Carignan, J., Libourel, G., 2006. Isotopic composition of Zn and Pb atmospheric depositions in an urban/periurban area of northeastern France. Environ. Sci. Technol. 40, 6594–6600.
- Collerson, K.D., Kamber, B.S., Schoenberg, R., 2002. Applications of accurate, high-precision Pb isotope ratio measurement by multi-collector ICP-MS. Chem. Geol. 188, 65–83.
- Dong, S., Ochoa Gonzalez, R., Harrison, R.M., Green, D., North, R., Fowler, R., Weiss, D., 2017. Isotopic signatures suggest important contributions from recycled gasoline, road dust and non-exhaust traffic sources for copper, zinc and lead in PM 10 in London. United Kingdom. Atmos. Environ. 165. 88–98.
- Dong, S., Weiss, D.J., Strekopytov, S., Kreissig, K., Sun, Y., Baker, A.R., Formenti, P., 2013. Stable isotope ratio measurements of Cu and Zn in mineral dust (bulk and size fractions) from the Taklimakan Desert and the Sahel and in aerosols from the eastern tropical North Atlantic Ocean. Talanta 114, 103–109.
- Guéguen, F., Stille, P., Dietze, V., Gieré, R., 2012. Chemical and isotopic properties and origin of coarse airborne particles collected by passive samplers in industrial, urban, and rural environments. Atmos. Environ. 62, 631–645.
- Gioia, S.M.C.L., Babinski, M., Weiss, D.J., Spiro, B., Kerr, A.A.F.S., Veríssimo, T.G., Ruiz, I., Prates, J.C.M., 2016. An isotopic study of atmospheric lead in a megacity after phasing out of leaded gasoline. Atmos. Environ. 149, 70–83.
- Gioia, S.M.C.L., Babinski, M., Weiss, D.J., Kerr, A.A.F.S., 2010. Insights into the dynamics and sources of atmospheric lead and particulate matter in São Paulo, Brazil, from high temporal resolution. Atmos. Res. 98, 478–485.
- Gioia, S.M.C.L., Weiss, D., Coles, B., Arnold, T., Babinski, M., 2008. Accurate and precise zinc isotope ratio measurements in urban aerosols. Anal. Chem. 80, 9776–9780.
- Herzog, G.F., Moynier, F., Albarède, F., Berezhnoy, A.A., 2009. Isotopic and elemental abundances of copper and zinc in lunar samples, Zagami, Pele's hairs, and a terrestrial basalt. Geochem. Cosmochim. Acta 73, 5884–5904.
- Kampa, M., Castanas, E., 2008. Human health effects of air pollution. Environ. Pollut. 151, 362–367.
- Komárek, M., Ettler, V., Chrastný, V., Mihaljevic, M., 2008. Lead isotopes in environmental sciences: a review. Environ. Int. 34, 562–577.
- Kumar, P., Andrade, M.D.F., Ynoue, R.Y., Fornaro, A., Freitas, E. D. De, Martins, J., Martins, L., Albuquerque, T., Zhang, Y., Morawska, L., 2016. New directions: from biofuels to wood stoves: the modern and ancient air quality challenges in the megacity of São Paulo. Atmos. Environ. 140, 364–369.
- Kumar, P., Morawska, L., Birmili, W., Paasonen, P., Hu, M., Kulmala, M., Harrison, R.M., Norford, L., Britter, R., 2014. Ultrafine particles in cities. Environ. Int. 66, 1–10.
- LAEI, 2010. London atmospheric emissions inventory (LAEI) 2010. Greater London authority (GLA). https://data.london.gov.uk/dataset/london-atmospheric-emissions-inventory-2010, Accessed date: 17 May 2018.

- Magnusson, O., 2014. Eurachem guide: the fitness for purpose of analytical methods. A laboratory guide to method validation and related topics. https://www.eurachem.org/index.php/publications/guides/mv, Accessed date: 14 May 2018.
- Maréchal, C., Télouk, P., Albarède, F., 1999. Precise analysis of copper and zinc isotopic compositions by plasma-source mass spectrometry. Chem. Geol. 156, 251–273.
- Martins, L.D., Andrade, M.F., Freitas, E.D., Pretto, A., Gatti, L.V., Albuquerque, E.L., Tomaz, E., Guardani, M.L., Martins, M.H.R.B., Junior, O.M.A., 2006. Emission factors for gas-powered vehicles traveling through road tunnels in São Paulo, Brazil. Environ. Sci. Technol. 40, 6722–6729.
- Mason, T.F.D., Weiss, D.J., Horstwood, M., Parrish, R.R., Russell, S.S., Coles, B.J., 2004. High-precision Cu and Zn isotope analysis by plasma source mass spectrometry Part 2. Correcting for mass discrimination effects. J. Anal. At. Spectrom. 19, 218–226.
- Mattielli, N., Petit, J.C.J., Deboudt, K., Flament, P., Perdrix, E., Taillez, A., Lanchon, J.R., Weis, D., 2009. Zn isotope study of atmospheric emissions and dry depositions within a 5 km radius of a Pb–Zn refinery. Atmos. Environ. 43, 1265–1272.
- Miranda, R.M., Andrade, M.F., Fornaro, A., Astolfo, R., Andre, P.F., Saldiva, P., 2012. Urban air pollution: a representative survey of $PM_{2.5}$ mass concentrations in six Brazilian cities. Air Qual. Atmos. Health 5, 63–77.
- Moeller, K., Schoenberg, R., Pedersen, R.B., Weiss, D., Dong, S., 2012. Calibration of the new certified reference materials ERM-AE633 and ERM-AE647 for copper and IRMM-3702 for zinc isotope amount ratio determinations. Geostand. Geoanal. Res. 36, 177–199
- Moynier, F., Pichat, S., Pons, M.L., Fike, D., Balter, V., Albarède, F., 2009. Isotopic fractionation and transport mechanisms of Zn in plants. Chem. Geol. 267, 125–130.
- Ochoa Gonzalez, R., Strekopytov, S., Amato, F., Querol, X., Reche, C., Weiss, D.J., 2016. New insights from zinc and copper isotopic compositions of atmospheric particulate matter from two major European cities. Environ. Sci. Technol. 50, 9816–9824.
- Ochoa Gonzalez, R., Weiss, D., 2015. Zinc isotope variability in three coal-fired power plants: a predictive model for determining isotopic fractionation during combustion. Environ. Sci. Technol. 49, 12560–12567.
- Peel, K., Weiss, D., Chapman, J., Arnold, T., Coles, B., 2008. A simple combined sample-standard bracketing and inter-element correction procedure for accurate mass bias correction and precise Zn and Cu isotope ratio measurements. J. Anal. At. Spectrom. 23, 103–110.
- Petit, J.C.J., Jong, J., Chou, L., Mattielli, N., 2008. Development of Cu and Zn isotope MC-ICP-MS measurements: application to suspended particulate matter and sediments from the Scheldt Estuary. Geostand. Geoanal. Res. 32, 149–166.
- from the Scheldt Estuary. Geostand. Geoanal. Res. 32, 149–166.
 Saiki, M., Santos, J.O., Alves, E.R., Genezini, F.A., Marcelli, M.P., Saldiva, P.H.N., 2014.
 Correlation study of air pollution and cardio-respiratory diseases through NAA of an atmospheric pollutant biomonitor. J. Radioanal. Nucl. Chem. 299, 773–779.
- Sivry, Y., Riotte, J., Sonke, J., Audry, S., Schafer, J., Viers, J., Blanc, G., Freydier, R., Dupre, B., 2008. Zn isotopes as tracers of anthropogenic pollution from Zn-ore smelters the Riou Mort–Lot River system. Chem. Geol. 255, 295–304.
- Sonke, J., Sivry, Y., Viers, J., Freydier, R., Dejonghe, L., Andre, L., Dupre, B., 2008. Historical variations in the isotopic composition of atmospheric zinc deposition from a zinc smelter. Chem. Geol. 252, 145–157.
- Sossi, P.A., Halverson, G.P., Nebel, O., Eggins, S.M., 2015. Combined Separation of Cu, Fe and Zn from Rock matrices and improved analytical protocols for stable isotope Determination. Geostand. Geoanal. Res. 39, 129–149.
- Souto-Oliveira, C.E., Babinski, M., Araújo, D.F., Andrade, M.F., 2018. Multi-isotopic fingerprints (Pb, Zn, Cu) applied for urban aerosol source apportionment and discrimination. Sci. Total Environ. 626, 1350–1366.
- Toutain, J.P., Sonke, J., Munoz, M., Nonell, A., Polvé, M., Viers, J., Freydier, R., Sortino, F., Joron, J.L., Sumarti, S., 2008. Evidence for Zn isotopic fractionation at Merapi volcano. Chem. Geol. 253, 74–82.
- Weis, D., Kieffer, B., Maerschalk, C., Barling, J., Jong, J. de, Williams, G.A., Hanano, D., Pretorius, W., Mattielli, N., Scoates, J.S., Goolaerts, A., Friedman, R.M., Mahoney, J.B., 2006. High-precision isotopic characterization of USGS reference materials by TIMS and MC-ICP-MS. G-cubed 7, 1–30.
- Widory, D., Liu, X., Dong, S., 2010. Isotopes as tracers of sources of lead and strontium in aerosols (TSP & PM2.5) in Beijing. Atmos. Environ. 44, 3679–3687.
- Widory, D., Roy, S., Moullec, Y.L., Goupil, G., Cocherie, A., Guerrot, K., 2004. The origin of atmospheric particles in Paris: a view through carbon and lead isotope. Atmos. Environ. 38, 953–961.
- World Health Organization, 2017. (WHO) website. http://www.who.int/phe/health_topics/outdoorair/en/, Accessed date: 10 January 2018.
- Yin, N.H., Sivry, Y., Benedetti, M.F., Lens, P.N.L., Van Hullebusch, E.D., 2015. Application of Zn isotopes in environmental impact assessment of Zn-Pb metallurgical industries: a mini review. Appl. Geochem. 64, 128–135.
- Young, E.D., Galy, A., Nagahara, H., 2002. Kinetic and equilibrium mass-dependent isotope fractionation laws in nature and their geochemical and cosmochemical significance. Geochim. Cosmochim. Acta. 66, 1095–1104.
- Zhu, Z., Jiang, S., Yang, T., Wei, H., 2015. International Journal of Mass Spectrometry Improvements in Cu – Zn isotope analysis with MC-ICP-MS: a revisit of chemical purification, mass spectrometry measurement and mechanism of Cu/Zn mass bias decoupling effect. Int. J. Mass Spectrom. 393, 34–40.